

Postprint of the Mechanism of Self-Propagating High-Temperature Synthesis in the Mg-B₂O₃-TiO₂ System

Authors: Wang Mingyuan, Li Junshou, Wu Xiaojuan, Li Su, Zhao Fang

Date: 2023-03-18T00:00:00+00:00

Abstract

Based on thermodynamic calculation results for the Mg-B₂O₃-TiO₂ system, a preliminary assessment of the reaction sequence was made; the Cu wedge combustion wave quenching method was then utilized to analyze the composition and morphology variations of products in various regions of the SHS reaction, thereby investigating the crystal synthesis and growth mechanism. Thermodynamic calculation results indicate that during the reaction process, Mg first reduces B₂O₃ to produce B and MgO, subsequently reduces TiO₂ to produce Ti and MgO, and finally, B combines with Ti to form TiB₂. With respect to intermediate products formed during the reaction, the probability of forming Ti₃O₅, Ti₂O₃, and TiO decreases sequentially. Experimental results demonstrate that at the combustion center, no intermediate products are generated due to relatively complete reaction; the temperatures at the secondary reaction center and edges remain relatively high, yielding small quantities of Ti₂O₃ and TiO; at the combustion bottom, incomplete reaction occurs due to lower temperatures, resulting in small quantities of Ti₃O₅, and the experimental results are consistent with thermodynamic analysis. During the reaction process, MgO nucleates and grows first, with some TiB₂ nucleating on MgO surfaces and forming fine particles as temperature increases; some TiB₂ nucleates independently between coarse MgO grains and grows into typical hexagonal crystal morphologies; the TiB₂ growth mechanism follows the L-S mechanism, with alternating enrichment of B and Ti generating typical hexagonal crystal morphologies.

Full Text

Preamble

Vol. 29 No. 1

CHINESE JOURNAL OF MATERIALS RESEARCH

January 2015

Self-propagating High Temperature Synthesis Mechanism of Mg-B₂O₃-TiO₂ System

WANG Mingyuan, LI Junshou, WU Xiaojuan, LI Su, ZHAO Fang
(Institute of Advanced Materials, Ordnance Engineering College, Shijiazhuang 050003, China)

Supported by National Natural Science Foundation of China No. 51172281.

ABSTRACT

The reaction sequence for the Mg-B₂O₃-TiO₂ system was determined through thermodynamic calculation. The composition and morphology evolution of products prepared by self-propagating high-temperature synthesis were then analyzed across different reaction zones using the Cu wedge combustion wave quenching method. The formation and growth mechanism of TiB₂ crystal grains was investigated as well. Thermodynamic calculations show that in the SHS reaction process, B and MgO were first obtained by reduction reaction between Mg and B₂O₃, then Ti and MgO were obtained by reduction reaction between Mg and TiO₂, and finally B reacted with Ti to form TiB₂. In this process, the possibility of intermediate product formation decreases in the following order: Ti₃O₅, Ti₂O₃, and TiO. Experimental results show that no intermediate products were detected in the combustion center, where the reaction was entirely complete; however, a small amount of Ti₂O₃ and TiO existed in zones near the center or at the edge, where the temperature was not high enough to complete the reaction; at the bottom zone of the combustion, a little Ti₃O₅ existed, where the temperature was too low for the reaction to complete. Therefore, thermodynamic prediction coincides well with experimental results.

It follows that during the SHS reaction process, MgO first nucleates and grows. TiB₂ may form through two pathways: in one pathway, TiB₂ nucleates on MgO crystals and then grows into tiny particles as temperature rises; in the other pathway, TiB₂ independently nucleates and grows into hexagonal crystals between large MgO crystals. The growth of TiB₂ follows a typical liquid-solid (L-S) mechanism; B and Ti alternatively gather and grow to form hexagonal crystals.

KEY WORDS inorganic non-metallic materials, TiB₂, SHS, combustion wave quenching method, synthesis mechanism

Introduction

Titanium diboride (TiB₂) is a non-oxide ceramic material and the most stable compound in the B-Ti binary system. It possesses high melting point, high hardness, excellent wear resistance, and good electrical conductivity, oxidation

resistance, and thermal shock resistance [1,2]. Numerous scholars have conducted substantial research on TiB_2 and its composite ceramics. Wang Weiming et al. [3] prepared TiB_2 using the $\text{Mg-B}_2\text{O}_3\text{-TiO}_2$ system and investigated the physical and chemical changes during reaction and the microstructure of TiB_2 powder. Fu Zhengyi [4] synthesized TiB_2 from B and Ti and studied the effects of raw material composition and diluent content on TiB_2 synthesis. Ma Aiqun [5] analyzed the phase diagram of the advantage region for TiB_2 synthesis mechanism and elucidated the reaction mechanism of carbothermal reduction for TiB_2 preparation. Li Zhenxi [6] studied the growth mechanism of borides in Ti-48Al+B alloys, specifically the growth mechanism of TiB_2 in alloys.

Our research group previously optimized the SHS process for preparing high-purity ultrafine TiB_2 powder. Building upon this work, the present study investigates the synthesis mechanism of ultrafine TiB_2 powder using the combustion wave quenching method [7]. Based on thermodynamic calculations of the $\text{Mg-B}_2\text{O}_3\text{-TiO}_2$ combustion reaction, the reaction sequence is first analyzed. Then, using Mg, B_2O_3 , and TiO_2 as raw materials, TiB_2 composite powder is synthesized via the Cu wedge combustion wave quenching method. By analyzing the composition and morphology evolution of reaction products in different regions of the Cu wedge, the synthesis and growth mechanism of TiB_2 powder is explored.

1. Thermodynamic Analysis of the $\text{Mg-B}_2\text{O}_3\text{-TiO}_2$ System

The Gibbs free energy for each reaction was calculated using the first approximation of the Gibbs free energy function to determine the reaction sequence and preliminarily predict the phases in each reaction zone [8]. The first approximation calculation equation is:

$$\Delta G = \Delta H - T\Delta S$$

Titanium has multiple valence states, so low-valence titanium compounds Ti_3O_5 , Ti_2O_3 , and TiO may appear during Ti reduction. The possible chemical reactions in the $\text{Mg-B}_2\text{O}_3\text{-TiO}_2$ system are:

- (1-1) $\text{TiO}_2 + 2\text{Mg} \rightarrow \text{Ti} + 2\text{MgO}$
- (1-2) $\text{TiO}_2 + \text{Mg} \rightarrow \text{TiO} + \text{MgO}$
- (1-3) $2\text{TiO}_2 + \text{Mg} \rightarrow \text{Ti}_2\text{O}_3 + \text{MgO}$
- (1-4) $3\text{TiO}_2 + \text{Mg} \rightarrow \text{Ti}_3\text{O}_5 + \text{MgO}$
- (1-5) $2\text{Mg} + \text{O}_2 \rightarrow 2\text{MgO}$
- (1-6) $\text{B}_2\text{O}_3 + 3\text{Mg} \rightarrow 2\text{B} + 3\text{MgO}$
- (1-7) $2\text{B} + \text{Ti} \rightarrow \text{TiB}_2$
- (1-8) $\text{TiO}_2 + \text{B}_2\text{O}_3 + 5\text{Mg} \rightarrow \text{TiB}_2 + 5\text{MgO}$

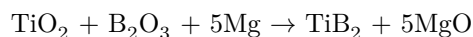
The Gibbs free energy for each reaction was calculated using the first approximation equation, yielding the temperature-dependent Gibbs free energy curves shown in [Figure 1: see original paper].

As shown in [Figure 1: see original paper], at room temperature the reaction sequence is (1-6), (1-9), (1-7), (1-8), (1-2), (1-5), (1-4), (1-3). When temperature is below 650 K, Mg reacts with O_2 first to form MgO (1-6) due to Mg's low melting point. When temperature exceeds 650 K, the reaction $TiO_2 + B_2O_3 + 5Mg \rightarrow TiB_2 + 5MgO$ (1-9) becomes most favorable. With non-uniform mixing and excluding reaction (1-9), Mg reacting with B_2O_3 to reduce B atoms (1-7) is most probable. As temperature increases, Mg reduces TiO_2 to obtain Ti atoms (1-2), then Ti and B atoms combine to form TiB_2 (1-8). During the SHS process, intermediate products Ti_3O_5 , Ti_2O_3 , and TiO may form, with their formation probability decreasing in that order.

According to [Figure 1: see original paper], MgO acts as a diluent that can reduce reaction rate and decrease the adiabatic combustion temperature, which benefits TiB_2 synthesis. To compensate for volatilization of some Mg and low-melting-point B_2O_3 , excess Mg and B_2O_3 can be added to the reaction system. Meanwhile, excess Mg and B_2O_3 can also reduce the adiabatic combustion temperature of the reaction system [9-11], facilitating TiB_2 synthesis.

2. Experimental Methods

Uniformly mixed raw materials were placed in a mold and compacted, then ignited with a tungsten wire to initiate the self-propagating high-temperature synthesis (SHS) reaction. The reaction equation is:



The Cu wedge combustion wave quenching method was employed to investigate the composition and morphology evolution during the SHS process, as illustrated in [Figure 2: see original paper]. Copper's excellent thermal conductivity absorbs substantial heat during reaction, causing the reaction to stop midway and enabling division of the combustion product into reaction zone, pre-reaction zone, and unreacted zone. Products from each zone were analyzed by XRD and SEM to explore morphology and composition changes during reaction.

The self-propagating combustion process is extremely complex, making synthesis mechanism investigation very difficult. Based on the reaction zone, pre-reaction zone, and unreacted zone shown in [Figure 2: see original paper], samples were taken from four specific locations—combustion center, combustion edge, second combustion center, and combustion bottom—as shown in [Figure 3: see original paper] for XRD and SEM analysis to reveal the crystal synthesis mechanism.

3. Results and Discussion

Figure 4: see original paper, (b), (c), and (d) show the XRD patterns from the

combustion center, combustion edge, second combustion center, and combustion bottom, respectively.

In the combustion center, due to slower heat dissipation and longer high-temperature residence time, reaction (1-9) proceeded more completely, yielding a two-phase product of $\text{TiB}_2 + \text{MgO}$. In the second combustion center, the reduced combustion wave propagation rate could not provide sufficient heat, affecting Ti reduction reactions and resulting in partial reduction of TiO_2 to intermediate products TiO and Ti_3O_5 . At the combustion edge, heat was rapidly absorbed by the Cu wedge, causing temperature to drop quickly and incomplete reduction of TiO_2 by Mg, producing the TiO phase. At the combustion bottom, rapid temperature decrease caused reaction termination, generating a small amount of Ti_3O_5 .

The combustion products from each zone were separated and ground into fine powder, as shown in [Figure 5: see original paper]. Most powder particles were approximately 50 nm in size, with some exceeding 100 nm and others below 10 nm. Due to manual grinding, the particle size distribution was relatively broad.

[Figure 6: see original paper] shows SEM images of the combustion bottom region. Some coarse particles exhibit cluster-like attachments of fine particles. The particles appear as irregular spheres with diameters mostly less than 30 nm. According to the nucleation work formula $\Delta G^* = 16\pi\sigma^3 T m^2 / (L m \cdot \Delta T)^2$, ΔG^* is inversely proportional to $(\Delta T)^2$, meaning greater undercooling requires smaller nucleation work. Therefore, at the lower-temperature combustion bottom, MgO should nucleate and grow first. TiB_2 nucleates on grown MgO crystals, but due to low temperature, TiB_2 nuclei cannot grow sufficiently, forming the morphology shown.

Figure 6: see original paper provides an enlarged view of the area in (a), revealing fine particles attached to some MgO crystal surfaces. Analysis indicates these fine particles are TiB_2 that did not have time to grow. [Figure 7: see original paper] presents a schematic diagram of the SHS reaction mechanism for the Mg- TiO_2 - B_2O_3 system. During ignition, B_2O_3 with the lowest melting point (723 K) melts first, followed by Mg with the second lowest melting point (922 K). TiO_2 with the highest melting point (2116 K) does not melt at ignition temperature and is thus surrounded by the Mg/ B_2O_3 melt. Combined with thermodynamic analysis, Mg first reacts with B_2O_3 in a liquid-liquid reaction to generate MgO and B [12-13], then Mg reacts with TiO_2 in a liquid-solid reaction to generate MgO and Ti, and finally Ti atoms combine with B atoms to form TiB_2 .

During reaction, MgO crystal nucleation and growth consume some heat, while the liquid-liquid reaction between Mg and B_2O_3 and the liquid-solid reaction between Mg and TiO_2 release substantial heat, causing rapid temperature increases in micro-regions that mutually trigger and sustain rapid combustion propagation [14]. MgO crystal nucleation and growth require significant heat, preventing some TiB_2 nucleating on MgO surfaces from growing sufficiently,

forming the morphology shown in Figure 6: see original paper. In other regions, higher local temperatures provide independent TiB_2 nuclei with adequate energy and growth space for various degrees of growth. Meanwhile, different heat dissipation conditions in various zones also significantly affect the resulting product regions.

[Figure 8: see original paper] shows SEM images of the combustion edge. Due to rapid heat loss at the Cu wedge edge, the temperature is lower than in the combustion center. However, MgO nucleation temperature is relatively low with small nucleation work, and continuous heat supply during combustion enables MgO to grow continuously at lower temperatures, forming large blocky crystals. Insufficient temperature restricts TiB_2 grain growth, which attaches to growing MgO as fine, elongated morphologies [15]. Since the initial reaction temperature remains higher than at the combustion bottom, a larger quantity of TiB_2 forms. Although TiB_2 grain growth is suppressed, TiB_2 still constitutes a major proportion, consistent with the XRD results.

[Figure 9: see original paper] shows SEM images of the second combustion center. Figure 9: see original paper reveals significantly grown TiB_2 grains with relatively uniform diameters around 200 nm. This occurs because the second combustion center has higher temperature and longer holding time than the edge and bottom, providing sufficient energy for TiB_2 and MgO grain growth. Figure 9: see original paper shows combustion product morphology at $30,000\times$ magnification, clearly displaying spherical, elongated, and hexagonal TiB_2 grains. TiB_2 belongs to the hexagonal C32 structure, where Ti atoms occupy the centers of the top and bottom faces and the 12 corners of the hexagonal unit cell, forming six pentahedral interstices fully occupied by six B atoms. This creates a crystal structure with alternating triangular Ti atom networks and hexagonal B atom networks. The linear symmetry along the cell axis and planar symmetry in the radial direction determine different growth tendencies along axial and radial directions. Tiny spherical particles formed during initial nucleation gradually grow as temperature increases, but varying surrounding thermodynamic conditions cause energy and temperature fluctuations around nuclei, resulting in different growth rates along radial or axial directions and forming various morphologies. Perforations on crystals may be left by impurity gas passage.

[Figure 10: see original paper] shows SEM images of the combustion center. The grain morphology in Figure 10: see original paper is more diverse than in the second combustion center. During combustion, the higher temperature and longer holding time in the center provided adequate growth time and space, supplying sufficient energy for continuous MgO growth. Some TiB_2 grains attached to or embedded in MgO crystals could not grow continuously because some heat was absorbed by MgO crystals, forming fine particles. Other TiB_2 grains located between coarse MgO crystals formed typical hexagonal morphologies due to favorable energy, composition, and temperature conditions, as shown in Figure 10: see original paper.

Based on growth traces on the side surfaces of hexagonal columnar TiB_2 crystals

in Figure 10: see original paper, ellipsoidal grains exhibit characteristic crystal growth. With radial (axial) preferential growth, tiny elongated or flaky particles form; elongated crystals grow into rod crystals, while flake crystals continue growing along the axial (radial) direction. [Figure 11: see original paper] illustrates the TiB_2 crystal growth mechanism. As shown, Mg first reduces B_2O_3 to obtain an enriched B layer, then Mg reduces TiO_2 to obtain an enriched Ti layer, forming flake crystals. Such layer-by-layer stacking eventually produces the typical hexagonal morphology [16].

Conclusions

1. In the SHS reaction of the Mg- B_2O_3 - TiO_2 system, Mg first reduces B_2O_3 to obtain B and MgO, then Mg reduces TiO_2 to obtain Ti and MgO, and finally B and Ti combine to generate TiB_2 . Incomplete reaction produces intermediate products Ti_3O_5 , Ti_2O_3 , and TiO, with formation probability decreasing in that order.
2. During SHS reaction of this system, MgO nucleates and grows first. Some TiB_2 nucleates and grows attached to MgO, forming fine spherical or elongated particles; other TiB_2 independently nucleates between coarse MgO crystals, growing into typical hexagonal morphologies.
3. The TiB_2 growth mechanism follows a typical liquid-solid (L-S) mechanism, where B and Ti alternately enrich and generate the typical hexagonal crystal morphology.

References

1. XIANG Xin, QIN Yan, Research progress of TiB_2 and its composite materials, *Journal of Ceramics*, 20(2), 112(1999)
2. ZOU Janping, SHEN Ming, Research progress of TiB_2 -based ceramic composites, *Scientific Research and Application*, 11, 7(2008)
3. WANG Weiming, FU Zhengyi, JING Mingji, YUAN Runzhang, Preparation of TiB_2 ceramic powders by self-propagating high temperature reduction synthesis, *Journal of Silicate*, 24, 52(1996)
4. FU Zhengyi, YUAN Runzhang, Research of the self-propagating high-temperature synthesis process of TiB_2 , *Journal of Silicate*, 23, 26(1995)
5. MA Aiqun, JIANG Mingxue, Phase diagram analysis of advantage area of TiB_2 synthetic reaction mechanism, *Journal of Chinese Non-ferrous Metals*, 21, 1409(2011)

6. LI Zhenxi, CAO Chunxiao, The growth mechanism of boride in Ti-48Al + B alloy, *Rare Metal Materials and Engineering*, 30(1), 19 (2001)
7. Rabiezadeh, A.M. Hadian, A. Ataie, Preparation of alumina/titanium diboride nano-composite powder by milling assisted sol-gel method, *Int. Journal of Refractory Metals and Hard Materials*, 31, 121 (2012)
8. Calka, D. Oleszak, Synthesis of TiB_2 by electric discharge assisted mechanical milling, *Journal of Alloys and Compounds*, 440, 346 (2007)
9. Riccardo Ricceri, Paolo Matteazzi, A fast and low-cost room temperature process for TiB_2 formation by mechanosynthesis, *Materials Science and Engineering*, 379, 341(2004)
10. ZHANG Yanan, DOU Zhihe, Research of growth mechanism TiB_2 micro powder prepared by self-propagating metallurgical method, *Journal of Inorganic Materials*, 21, 583(2006)
11. ZHANG Haijun, LI Faliang, Preparation and microstructure evolution of diboride ultrafine powder by sol-gel and microwave carbothermal reduction method, *J Sol-Gel Sci Technol*, 45, 205(2008)
12. LIU Hongwei, ZHANG Long, WANG Jangjian, DU Xingkan, Preparation of TiB_2 -TiC composite ceramics by self-reacting injection forming, *Journal of Materials Research*, 22(3), 274(2008)
13. Kiyotaka Matsuura, Yuki Obara, Keisuke Kojima, Combustion synthesis of boride particle dispersed hard metal from elemental powders, *Int. Journal of Refractory Metals & Hard Materials*, 27, 376 (2009)
14. ZHANG Lei, YANG Bing, CHEN Weina, ZHANG Xiaonan, Effects of TiB_2 particles on the grain growth behavior of semi-solid aluminum matrix composites, *Casting Technology*, 31(8), 991(2010)
15. GAO Wenli, ZHANG Hu, ZHANG Erlin, ZENG Songyan, Surface morphology and formation mechanism of primary TiB_2 crystal in Ti-Al-B alloy, *Materials Science and Technology*, 10(4), 387(2002)
16. GAO Wenli, ZHANG Hu, ZHANG Erlin, ZENG Songyan, The main form of the microstructure of TiB_2 in Ti-Al-B alloy, *Casting Technology*, 3, 176(2003)

Note: Figure translations are in progress. See original paper for figures.

Source: ChinaXiv – Machine translation. Verify with original.